A Neutral Technetium-99m Complex for Myocardial Imaging

Rama K. Narra, Adrian D. Nunn, Bruce L. Kuczynski, Tom Feld, Paul Wedeking, and William C. Eckelman

The Squibb Institute for Medical Research, New Brunswick, New Jersey

Technetium-99m-CDO-MeB ((Bis[1,2-cyclohexanedione-dioximato(1-)-O]-[1,2-cyclohexanedione dioximato(2-)-O]methyl-borato(2-)-N,N′,N″,N‴,N⁗,N⁗′)-chlorotechnetium) belongs to a family of compounds generally known as boronic acid adducts of technetium dioxime complexes (BATOs). It has an intrinsic affinity for the myocardium, with negligible lung activity and rapid blood clearance. The uptake of 3.44 %ID in rat heart at 1 min postinjection for [^{99m}Tc]CDO-MeB versus 3.03% for ^{201}Tl indicates high extraction of [^{99m}Tc]CDO-MeB by the myocardium. In dogs an ischemic defect is clearly seen in SPECT images obtained 10 min after injection of [^{99m}Tc]CDO-MeB. Tissue distribution data in rats show that [^{99m}Tc]CDO-MeB is excreted primarily in the feces and to a lesser extent in the urine. Approximately 80% of the activity is excreted within 24 hr after injection.

J Nucl Med 30:1830–1837, 1989

Myocardial perfusion imaging with thallium-201 (^{201}Tl) is a routine procedure for noninvasive diagnosis of myocardial infarction and ischemia (*1–4*). Since technetium-99m (^{99m}Tc) radiopharmaceuticals have usually replaced those containing a different radionuclide because of the availability of ^{99m}Tc, there is considerable interest in developing ^{99m}Tc-labeled myocardial imaging agents. Initial efforts were focused on producing ^{99m}Tc cationic complexes with the expectation that a compound with a positive charge would mimic the biologic behavior of the thallous ion which is taken up by the Na^+/K^+ ATPase pump (*5–6*). The Tc(III) cationic complexes tr-[^{99m}Tc(DMPE)$_2$Cl$_2$]$^+$ (DMPE = 1,2-bis(dimethylphosphino)ethane) and tr-[^{99m}Tc(DEPE)$_2$Cl$_2$]$^+$ (DEPE = 1,2-bis(diethylphosphino)ethane) showed good myocardial uptake in rats and dogs but failed to produce clinically efficacious images in man because there was insufficient activity in the heart (*7–10*). The first Tc(I) cationic complexes also failed to produce satisfactory myocardial images in humans after giving good animal images. The clearance from the blood in man of the Tc(I) complexes [^{99m}Tc(DMPE)$_3$]$^+$, [^{99m}Tc(POM-POM)$_3$]$^+$ (POM-POM = 1,2-bis(dimethoxyphosphino)ethane) and [^{99m}Tc(TMP)$_6$]$^+$ (TMP = trimethylphosphite) is very slow and obscures the myocardial activity (*11*). The Tc(I) complex [^{99m}Tc(TBIN)$_6$]$^+$ (TBIN = t-butylisonitrile), however, behaves differently from the Tc(I) phosphino complexes in that it rapidly clears from the blood but accumulates in the lung. It shows unfavorable heart/lung ratios for some hours after injection (*12*).

A new Tc(I) cationic complex ^{99m}Tc hexakis-methoxyisobutyl isonitrile (MIBI) is showing promise for myocardial perfusion imaging in man (*13*).

We have developed a new class of neutral, lipophilic technetium containing complexes for myocardial imaging in humans. These complexes are generally known as boronic acid adducts of technetium dioxime complexes (BATOs) (*14*). They are easily prepared by template synthesis from vicinal dioximes and a boronic acid. Details of their chemistry are described elsewhere (*15–16*). They are heptacoordinate complexes in which the technetium is bound to the six nitrogens of the three vicinal dioximes and an axial chloride ligand. The oximes are capped at one end through the oxygens by a tetrahedrally coordinated boron atom and at the other end the three oxygens are held together by a two proton bridge. We report the data from preclinical testing of [^{99m}Tc]CDO-MeB; a BATO in which the oximes are cyclohexanedione dioxime and a methyl group occupies the fourth coordinate site on the boron.

Received Dec. 1, 1988; revision accepted July 21, 1989.

For reprints contact: A. D. Nunn, The Squibb Institute for Medical Research, P.O. Box 191, New Brunswick, NJ 08903-0191.

MATERIALS AND METHODS

The [^{99m}Tc]CDO-MeB was prepared from a lyophilized kit by the addition of 1 ml pertechnetate containing 10 to 100

mCi ^{99m}Tc followed by heating at 100°C for 15 min, and then cooling to room temperature. Each vial contains 1,2-cyclohexanedione dioxime (14.1 μmol) and methyl boronic acid (33.3 μmol) as active ingredients and anhydrous stannous chloride (0.26 μmol) as a reducing agent. Other excipients in the kit are sodium chloride (171 μmol), diethylenetriaminepentaacetic acid (5.1 μmol), anhydrous citric acid (46.7 μmol) and gamma cyclodextrin (38.6 μmol) required to achieve a stable preparation with high radiochemical yield. The radiochemical purity (RCP) of each preparation was measured either by reversed-phase high performance liquid chromatography (HPLC) or by paper chromatography. The HPLC system consists of a Hamilton PRP-1 column (150×4.1 mm) eluted with 90%ACN-10% 0.1 *M* ammonium acetate buffer, pH 4.6, at a flow rate of 2.0 ml/min. An on line NaI(Tl) detector in conjunction with a high voltage power supply (Tennelec #TC948), a linear amplifier (Tennelec #TC211A) and a single channel analyzer (Tennelec #441) was used to measure the radioactivity. All equipment was validated before use.

Paper chromatography was used to separate the ^{99m}Tc-labeled CDO-MeB complexes from pertechnetate and other non lipophilic impurities. A 1–5 μ sample was applied to two 1.3 cm × 10 cm Whatman 31ET paper strips 2 cm from an end. The strips were immediately developed one with 0.9% NaCl and the other with acetone/0.9% NaCl(50:50 v/v) solvent by the ascending technique in small jars. Each chromatogram was then divided into origin and front sections as shown in Figure 1. All sections were assayed for radioactivity using a well counter. Pertechnetate and reduced hydrolyzed fractions of ^{99m}Tc were estimated using:

$$\%\ ^{99m}TcO_4^-(FTc) = \frac{F_s}{F_s + O_s} \times 100,$$

where F_s and O_s are respectively the radioactivities in the front and origin sections of the strip developed in saline, and

$$\%\text{Reduced Hydrolyzed } ^{99m}\text{Tc (RHTc)} = \frac{O_{a/s}}{F_{a/s} + O_{a/s}} \times 100,$$

where $F_{a/s}$ and $O_{a/s}$ are respectively the activities in the front and origin sections of the strip developed in acetone/saline solvent.

The RCP defined as the percent of total activity associated with the CDO-MeB complex is calculated as:

$$\%RCP = (100 - (FTc + RHTc)).$$

The other compounds, ^{99m}Tc[$DMPE_2Cl_2$]$^+$ ^{99m}Tc-[DMPE]$_3^+$, ^{99m}Tc[hexakis(t-butylisonitrile)]$^+$(TcBIN), were prepared and tested for RCP by published methods and had RCPs >90% (*17–18*).

All imaging studies were performed using an Elscint Apex 409 camera equipped with either a HRES or pinhole collimator.

Radioactivity in tissue samples was counted using either a Searle Autogamma Counter Model 1197 or LKB 1282 Compugamma counter.

ANIMAL STUDIES

Myocardial Uptakes of [^{99m}Tc]CDO-MeB and ^{201}Tl in Rats

The myocardial uptake of [^{99m}Tc]CDO-MeB and thallium-201(^{201}Tl) was measured in male Sprague-Dawley rats (225–275 g), at 1 and 5 min after co-injection, or separate injections, of the two agents.

For each study the animal was anesthetized with an i.p. injection of nembutal at a dose of 50 mg/kg. The jugular vein was exposed and 0.1 ml of the test sample containing ^{201}Tl(5–15 μCi) and [^{99m}Tc]CDO-MeB (10–30 μCi) was injected. At the designated time, the animal was killed. The heart was removed and assayed for both [^{99m}Tc]CDO-MeB and ^{201}Tl activities against a 1% standard.

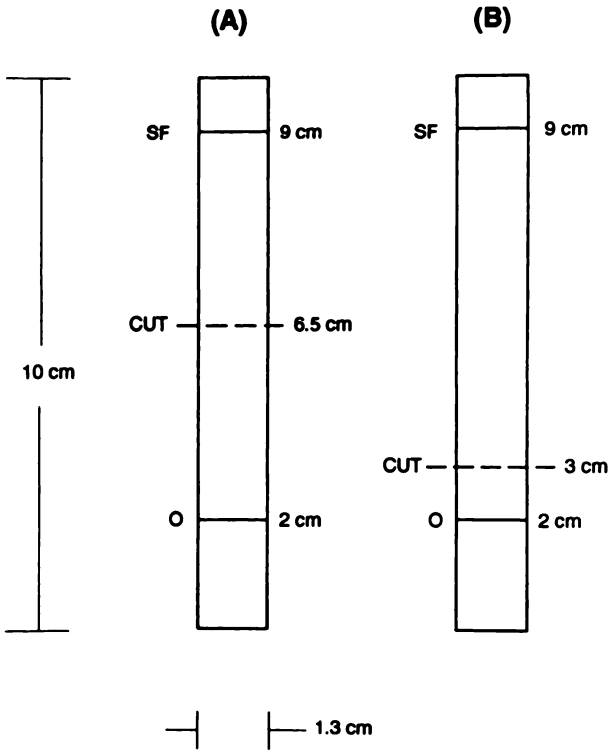

FIGURE 1
Paper chromatography system using Whatman 31ET as the stationary phase. Solvent "saline" in (A) separates the pertechnetate from labeled lipophilic complexes and insoluble reduced hydrolyzed technetium. Solvent "acetone/saline" in (B) separates the reduced hydrolyzed technetium from labeled lipophilic complexes and pertechnetate.

Myocardial Uptakes of [^{99m}Tc]CDO-MeB, Tc(DMPE)$_2Cl_2^+$, Tc(DMPE)$_3^+$ and TcBIN in Rats and Guinea Pigs

The myocardial uptakes of [^{99m}Tc]CDO-MeB, Tc(DMPE)$_2Cl_2^+$, Tc(DMPE)$_3^+$ and TcBIN were measured at 5 min after injection in rats (225–275 g) and guinea pigs (350–450 g). The rats were anesthetized as described above and the guinea pigs were anesthetized with pentobarbital at an i.p. dose of 30 mg/kg. A dose of 0.1 ml containing 10–30 μCi of the test sample was administered to each animal via the jugular vein. At 5 min after injection, the animal was killed. The heart was then excised and assayed for ^{99m}Tc activity against a 1% standard.

Biodistribution in Rats

The time course of organ distribution and clearance of [^{99m}Tc]CDO-MeB was examined in rats at 0.017, 0.10, 0.25,

0.5, 1, 2, 4, 8, 12, 18 and 24 hr after injection. Eleven groups of five male Sprague-Dawley rats weighing between 100 and 155 g were used (small animals were used to facilitate the counting of the whole carcass required for this study). Each rat was anesthetized with nembutal sodium at an i.p. dose of 50 mg/kg. The penis of each rat in the first five groups was ligated immediately prior to injection. The jugular vein was exposed via an incision and each rat was injected with 0.1 ml containing 4–70 μCi of [^{99m}Tc]CDO-MeB (longer residence groups received higher activity). Following injection, the incisions of rats in the 2 hr and longer residence groups were closed and then the rats were placed in individual metabolic cages to facilitate collection of urine and feces.

Ten minutes before the designated time each rat was reanesthetized if necessary. Approximately 3 ml of blood was withdrawn via a cardiac puncture and the animal was killed by exsanguination. The urine was removed from the bladder and combined with urine, if any, collected from the metabolic cage. The feces were treated separately. The organs of interest were dissected and transferred to counting tubes; the heart was emptied free of blood and rinsed in water before transferring to counting tubes. The blood, urine, feces, and carcass were also placed in counting tubes and assayed against a 1% standard.

A sample of blood was drawn into a capillary tube and centrifuged. The capillary was broken at the RBC-plasma interface and the activity in both fractions was assayed.

Imaging Studies in Dogs

Four beagle dogs of either sex weighing between 9 and 13 kg were used. SPECT imaging of the myocardium were performed; each in two normal and in two ischemic dogs. Each animal was anesthetized with an i.v. dose of 30 mg/kg nembutal sodium. Catheters were placed in a saphenous vein and in a femoral artery. The venous catheter was used to administer the test sample [^{99m}Tc]CDO-MeB, and maintenance doses of anesthesia; whereas the arterial catheter was used to withdraw blood.

Acute ischemia in the dogs was created by occlusion of the left anterior descending (LAD) coronary artery using the following procedure. After anesthesia, the animal was intubated, and ventilated with room air using a Harvard respirator. A left thoracotomy was performed via the fifth intercostal space and the myocardium was suspended in a pericardial cradle. The LAD was isolated proximal to the first major diagonal branch. A silk suture (2-0) was placed around the LAD (~1 cm below the bifurcation of the circumflex branch) and was used to occlude the LAD. Immediately after LAD occlusion a dose of 6 to 10 mCi [^{99m}Tc]CDO-MeB in 1 ml was administered i.v. A 360° rotation was used to collect 120 (3°) projections in 10 or 15 min in a 128 × 128 matrix starting at 10 min after injection.

Time-Activity Curves of Normal Rat, Guinea Pig and Dog Hearts

Time-activity (T/A) curves of the heart were obtained in four rats, six guinea pigs, and four dogs. A pinhole collimator was used for the rat and guinea pig acquisitions, whereas a HRES collimator was used for the dog studies. The animals were prepared as described above. Each animal was placed supine under the camera. After administering 1.5–3.0 mCi (0.1–2.0 ml) of [^{99m}Tc]CDO-MeB, dynamic imaging of the heart in the anterior view was performed for 60 min collecting 1 frame/min in a 128 × 128 matrix. At the end of the acquisition the animal was killed, the heart excised and assayed for ^{99m}Tc activity against a suitable standard. A fast study grouping of ten images, from 2–12 min, of the dynamic acquisition was generated and the composite image was used to construct a whole heart region of interest (ROI). Using this ROI, a time/activity histogram (counts/ROI vs. Time) of the heart was generated for the 60-min acquisition. The measured activity in the heart at 60 min expressed as percent injected dose (% ID), and the corresponding histogram data point were used as the basis to express the entire histogram data in units of %ID and a new heart T/A curve (%ID vs. Time) was constructed. Time-activity curves of the heart were analyzed by nonlinear regression analysis using RS/1 software (BBN Software Products Corporation, Cambridge, MA).

Blood Clearance of [^{99m}Tc]CDO-MeB

The blood clearance data in the three animal species were obtained by collecting duplicate exact aliquots of 10 μl blood via the arterial catheter at 1, 2, 3, 4, 5, 10, 15, 30, 45, and 60 min postinjection. The samples were then assayed against a measured 0.02% ^{99m}Tc standard. The percent injected dose present in the blood pool of each animal was calculated using the blood volumes of 65 ml/kg for rat and dog, and 75 ml/kg for guinea pig.

Dosimetry

The radiation dosimetry to humans from injection of [^{99m}Tc]CDO-MeB was estimated based on rat in vivo distribution data. The contribution of radioactivity of blood in organs to the radiation dose to the organs is assumed negligible as the activity is cleared fast from the blood. The time-activity data were used to determine the cumulative activities in various source organs. Absorbed doses in target organs were calculated using the published "S" factors (*19–20*).

RESULTS

Figure 2 shows a typical HPLC radiochromatogram of [^{99m}Tc]CDO-MeB prepared from a lyophilized kit. The major peak at ~3 min is the [^{99m}Tc]CDO-MeB. The RCP of the preparation is always greater than 90% and is stable for 6 hr. The paper chromatography also gives an RCP >90%. The RCPs of three kit preparations measured by both methods are 94.5, 93.6, 93.9 by HPLC and 93.8, 93.7, 93.8 by paper chromatography, respectively.

Table 1 gives the myocardial uptakes of [^{99m}Tc]CDO-MeB and ^{201}Tl in rats (225–250 g) at 1 and 5 min after injection. The heart uptake of 3.44% ID for [^{99m}Tc]CDO-MeB vs. 3.03% for ^{201}Tl at 1 min postinjection suggests high extraction of [^{99m}Tc]CDO-MeB by the rat myocardium. The drop in myocardial activity from 3.44% ID at 1 min to 2.08% ID by 5 min shows that the net clearance of [^{99m}Tc]CDO-MeB from the myocardium is faster than that of ^{201}Tl.

The rat and guinea pig heart uptakes at 5 min postinjection (PI) of $Tc(DMPE)_2Cl_2^+$, $Tc(DMPE)_3^+$, TcBIN and [^{99m}Tc]CDO-MeB are given in Table 2. The t-test

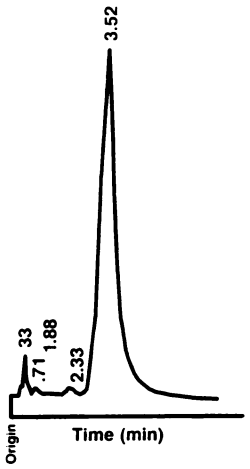

FIGURE 2
A typical HPLC chromatogram of [^{99m}Tc]CDO-MeB using a Hamilton PRP-1 column and eluted with 90%ACN-10% ammonium acetate buffer, pH 4.6 at a flow rate of 2 ml/min. The percent activity in the main peak is >90%.

showed the mean myocardial uptake of [^{99m}Tc]CDO-MeB in rats at 5 min postinjection of 2.08 (Table 1, n = 13) is not significantly different from that of 1.81 (Table 2, n = 3). The rat model gave similar uptakes for all the four compounds while the guinea pig model gave poor uptakes for $Tc(DMPE)_2Cl_2^+$, $Tc(DMPE)_3^+$ and good uptake for TcBIN and [^{99m}Tc]CDO-MeB.

The results of the tissue distribution study in rats (100–125 g) are given in Table 3. In this group of rats the mean myocardial uptake at 1 min postinjection is 4.64 ± 0.49% ID. The t-test indicated that this is significantly different, ($p < 0.01$) from that of 3.44% ID in rats of 225–250 g (Table 1, n = 8). This could be because of the differences in the cardiac output and/or the fractional cardiac output to the myocardium among the two groups; the younger rats having relatively higher flow to the myocardium than the older rats.

The clearance of [^{99m}Tc]CDO-MeB from blood is rapid; at 1 min postinjection (PI) <4% of the dose is present in the blood and ~1.0% of the dose is associated with RBCs. The uptake in the heart peaks at 4.6% ID at 1 min PI, and by 15 min it drops to ~1%. At 1 min PI the liver contains the highest activity; this is also the major organ of excretion.

Technetium-99m CDO-MeB is excreted primarily in the feces and, to a lesser extent, in the urine. During the 24 hr after administration, approximately 68% of

TABLE 1
Heart Uptake (%ID) of ^{201}Tl and [^{99m}T]CDO-MeB in Rats

Time	^{201}Tl	[^{99m}T]CDO-MeB
1 min	3.03 ± 0.13 (n = 6)*	3.44 ± 0.32 (n = 8)
5 min	3.30 ± 0.32 (n = 10)	2.08 ± 0.29 (n = 13)

* Mean ± s.d. for (n) the number of animals tested.

TABLE 2
Mean Percent Injected Dose in the Myocardium at 5 min Postinjection

Compound	Rat	Guinea pig
$Tc(DMPE)_2Cl_2+$	2.69 (1.99–3.17)*	0.48 (0.39–0.47)
$Tc(DMPE)_3+$	1.55 (1.23–1.87)	0.60 (0.45–0.80)
TcBIN	2.10 (2.03–2.16)	1.88 (1.45–2.30)
CDO-MeB	1.81 (1.39–2.23)	1.77 (1.35–2.51)

* Represents the range as only three animals were used in each group of this study.

the dose is excreted in the feces and ~13% in the urine. Thus, the activity remaining in the whole body at 24 hr is <19%; when corrected for decay this represents less than 2% of the administered dose. The radiation dosimetry estimations based on data in Table 3 are shown in Table 4. The estimations show that the small and large intestines are the target organs and will receive, respectively, 170 and 160 mrad/mCi [^{99m}Tc]CDO-MeB injected. The liver, kidneys, and ovaries each receive ~50 mrad/mCi. Thus a dose of up to 30 mCi [^{99m}Tc]CDO-MeB may be administered per clinical study either in single or divided administrations, based on these animal data. This assumes a maximum dose of 5000 mrad to any single organ.

The blood T/A data, with the assumption that 100% of the activity was present at T = 0, were analyzed by nonlinear regression analysis using RS/1 software. The unweighted data were fitted to both bi- and tri-exponential functions of the form:

$$Y_{Blood} = A\ e^{-\alpha t} + B\ e^{-\beta t} \text{ and}$$

$$Y_{Blood} = A\ e^{-\alpha t} + B\ e^{-\beta t} + C\ e^{-\gamma t},$$

where the coefficients A, B and C represent the activities associated with the clearance/growth components; α, β, and γ are the clearance or growth rate constants.

To examine which of the two functions is a superior fit, the F-ratio test was used (*21*). The F-test was performed using a weighting factor:

$$W_i = 1/(Y_i)^2 \text{ and}$$

$$\text{(weighted residual)} = \text{(unweighted residual)} * (\text{weight})^{1/2}$$

The tri-exponential function was found to be superior to the bi-exponential function.

The blood T/A curves in dogs and guinea pigs clearly showed a growth component (negative values of γ) presumably due to clearance into blood from the major organs. In rats the growth component is not evident but there is a third component with much longer clearance half-time.

The blood clearance curves of [^{99m}Tc]CDO-MeB, average percent injected dose in total blood versus time,

TABLE 3

Average Distribution of Radioactivity in Tissues of Rats After Intravenous Administration of [^{99m}Tc]CDO-MeB Expressed as % Injected Dose/Total Tissue*

	Residence time (hr) 0.017		Residence time (hr) 0.1		Residence time (hr) 0.25		Residence time (hr) 0.5		Residence time (hr) 1.0		Residence time (hr) 2.0	
Tissue	Mean	s.d.	Mean	s.d.	Mean	s.d.	Mean	s.d.	Mean	s.d.	Mean	s.d.
Whole blood	3.93	0.28	2.65	0.18	2.27	0.26	2.10	0.32	1.71	0.12	1.60	0.15
RBCs‡	1.11	0.14	0.69	0.04	0.91	0.10	0.85	0.03	0.81	0.09	0.97	0.14
Plasma‡	2.82	0.28	1.96	0.17	1.36	0.24	1.25	0.30	0.90	0.05	0.63	0.10
Heart	4.64	0.49	1.85	0.42	1.00	0.11	0.67	0.07	0.45	0.05	0.36	0.04
Lungs	4.42	0.83	1.39	0.15	1.23	0.18	0.94	0.08	0.86	0.07	0.80	0.10
Brain	0.77	0.11	0.47	0.02	0.44	0.02	0.37	0.04	0.37	0.06	0.36	0.07
Liver	23.73	1.39	24.71	1.47	24.10	1.13	21.86	1.65	16.70	2.03	15.35	1.50
Stomach	2.07	0.15	1.53	0.19	1.32	0.14	1.88	0.69	1.27	0.19	2.65	1.18
Sm. intestine	10.89	1.28	8.99	0.24	13.26	1.63	21.24	4.02	28.79	1.04	38.80	2.66
Lg. intestine	2.38	0.34	1.73	0.11	1.75	0.12	1.74	0.07	1.71	0.13	1.97	0.06
Bladder	0.06	0.04	0.15	0.10	0.12	0.02	0.15	0.05	0.12	0.04	0.23	0.34
Testes	0.26	0.06	0.29	0.05	0.29	0.03	0.28	0.04	0.32	0.11	0.26	0.04
Spleen	1.31	0.21	0.65	0.12	0.62	0.13	0.44	0.03	0.35	0.05	0.30	0.04
Pancreas	1.46	0.12	0.77	0.11	0.67	0.06	0.60	0.18	0.40	0.13	0.30	0.05
Kidneys	7.81	1.09	4.20	0.56	3.07	0.31	2.16	0.20	2.01	0.13	1.76	0.07
Adrenals	0.22	0.04	0.30	0.08	0.27	0.06	0.16	0.02	0.09	0.02	0.07	0.02
Thymus	0.40	0.11	0.49	0.12	0.43	0.10	0.34	0.05	0.20	0.07	0.16	0.05
Thyroid	0.19	0.03	0.10	0.02	0.10	0.02	0.08	0.01	0.06	0.01	0.05	0.01
Eyes	0.06	0.01	0.04	0.01	0.04	0.01	0.03	0.00	0.03	0.02	0.02	0.00
Bone§	8.90	0.61	6.75	0.35	6.47	0.20	5.01	0.38	5.28	0.40	5.12	0.16
Feces	0.00	0.00	0.00	0.00	0.00	0.00	0.00	0.00	0.00	0.00	0.00	0.00
Urine	0.00	0.00	0.31	0.14	0.85	0.15	1.95	0.17	3.38	0.71	5.21	0.73
Carcass	43.12	0.99	43.74	3.77	41.24	4.96	39.69	3.62	33.81	2.93	28.45	2.44
Total recovery	108.79		95.11		93.80		97.47		93.80		99.78	

	Residence time (hr) 4.0		Residence time (hr) 8.0		Residence time (hr) 12.0		Residence time (hr) 16.0		Residence time (hr) 24.0	
Tissue	Mean	s.d.	Mean	s.d.	Mean	s.d.	Mean	s.d.	Mean	s.d.
Whole blood	1.30	0.14	0.94	0.14	0.96	0.12	0.84	0.06	0.72	0.13
RBCs‡	0.77	0.06	0.56	0.09	0.71	0.12	1.24	0.17	0.62	0.07
Plasma‡	0.53	0.12	0.38	0.04	0.25	0.02	0.28	0.16	0.10	0.10
Heart	0.20	0.04	0.14	0.02	0.10	0.01	0.08	0.01	0.07	0.01
Lungs	0.60	0.13	0.35	0.05	0.22	0.02	0.17	0.01	0.17	0.03
Brain	0.30	0.05	0.29	0.06	0.21	0.02	0.21	0.02	0.20	0.05
Liver	9.73	1.22	8.40	0.84	6.85	0.54	6.06	0.45	4.27	0.51
Stomach	0.89	0.32	0.45	0.37	1.30	2.45	1.68	0.82	0.17	0.09
Sm. intestine	45.30	9.59	7.53	2.33	3.22	0.94	5.07	2.10	1.32	0.45
Lg. intestine	12.60	11.42	55.66	17.58	28.03	5.01	6.65	4.54	2.60	0.80
Bladder	0.07	0.06	0.05	0.02	0.02	0.01	0.01	0.01	0.01	0.00
Testes	0.23	0.05	0.12	0.04	0.12	0.01	0.12	0.01	0.06	0.04
Spleen	0.27	0.05	0.16	0.05	0.12	0.01	0.08	0.01	0.09	0.02
Pancreas	0.22	0.06	0.11	0.02	0.08	0.01	0.05	0.01	0.04	0.01
Kidneys	1.83	0.11	1.89	0.09	1.80	0.11	1.45	0.19	1.31	0.17
Adrenals	0.04	0.01	0.02	0.01	0.01	0.00	0.01	0.00	0.01	0.00
Thymus	0.13	0.01	0.08	0.01	0.06	0.01	0.04	0.01	0.04	0.00
Thyroid	0.03	0.01	0.02	0.00	0.01	0.00	0.02	0.00	0.01	0.00
Eyes	0.01	0.00	0.01	0.00	0.01	0.00	0.01	0.00	0.01	0.00
Bone§	2.70	0.36	0.52	0.13	1.28	0.07	0.97	0.02	0.24	0.05
Feces	0.12	0.08	9.04	19.16	35.03	7.18	62.00	5.44	68.09	5.27
Urine	8.67	3.21	7.68	0.80	12.94	1.67	12.55	1.57	13.07	1.79
Carcass	21.03	2.87	8.95	1.32	10.87	2.58	8.61	0.88	6.35	0.95
Total recovery	104.82		102.43		102.61		106.68		98.84	

TABLE 4
Estimations of Absorbed Dose Following i.v. Administration of [^{99m}Tc]CDO-MeB to Humans

Organ	Dose (mrad/mCi inj.)
Heart wall	13.0
Lungs	9.8
Brain	2.7
Liver	57.0
Stomach	32.0
Sm. intestine	170.0
Lg. intestine	160.0
Bladder	18.0
Testes	29.0
Spleen	19.0
Pancreas	29.0
Kidneys	49.0
Adrenals	27.0
Thyroid	12.0
Bone	9.3
Red-marrow	25.0
Whole body	15.0
Eyes	12.0
Ovaries	51.0

in rats, guinea pigs, and dogs along with their respective fit-functions are shown in Figure 3. In all three species the blood clearance is fast; more than 90% of the activity is cleared by 3 min after injection.

The heart T/A curves of the three species were best fitted to a bi-exponential function. The heart T/A curves of rat, guinea pig, and dog along with their respective fit-functions are shown in Figure 4. In these animals approximately two-thirds of the heart activity is cleared through a fast component and the remainder by a slow component. The half-times of the fast and slow clearance components calculated from the individual animal T/A data, respectively, are 3.6 ± 0.6 and 98.7 ± 15.3 min in dogs (n = 4); 1.0 ± 0.4 and 56.3 ± 9.6 min in guinea pigs (n = 6); and 1.7 ± 0.4 and 52.6 ± 5.8 (n = 4) in rats.

Single photon emission computed tomographic (SPECT) images of normal and regionally ischemic dog hearts involving the left descending coronary artery are shown in Figure 5. Transaxial reconstructions of 1 pixel slice width at 4× zoom were prepared from the SPECT acquisitions. From the transaxial sections, 15 3-pixel width oblique frontal (short axis) slices of the whole heart were constructed. The perfusion defect is evident in both the ischemic regions of the hearts (frames 3 to 10 in (B) and (C) of Figure 5).

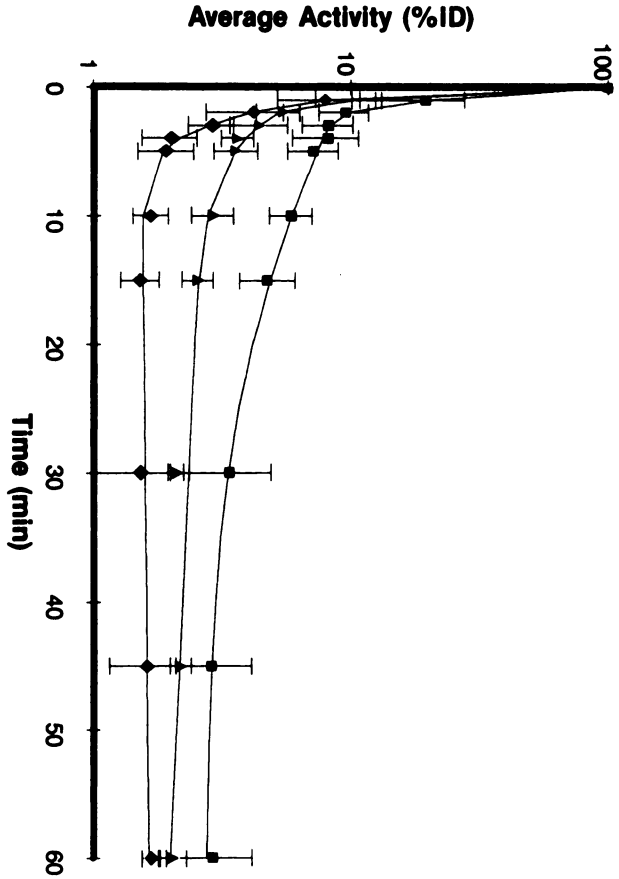

FIGURE 3
Blood clearance of [^{99m}Tc]CDO-MeB in dog, guinea pig, and rat; average activity (% ID) in total blood versus time (min) is shown. Dog (n = 4), ■; guinea pig (n = 4), ◆; and rat (n = 4), ▲; with respective fit functions of: $90.40\ e^{-2.13t} + 7.10\ e^{-0.075t} + 2.51\ e^{-(-0.0029)t}$; $88.17\ e^{-4.18t} + 10.29\ e^{-0.691t} + 1.54\ e^{-(-0.0012)t}$; and $92.63\ e^{-3.10t} + 4.60\ e^{-0.332t} + 2.77\ e^{-0.0054t}$.

DISCUSSION

The radiochemical purity of SQ 30217 prepared from lyophilized kits is always >90% and it is stable for 6 hr. Both HPLC and PC methods gave almost identical results. The paper chromatography is an easy, fast, and convenient method which could be used in any nuclear medicine department. However, it is to be noted that a sample of as small as one microliter from a kit containing 50 mCi ^{99m}Tc SQ 30217 will saturate the NaI(Tl) crystal of the well counter. Thus it is advisable to assay the chromatography strips in the proper geometry.

*Values shown are Mean and s.d. for five rats.

† The total % of the dose in blood was calculated by assuming that blood comprised 6.5% of the total body weight.

‡ Values calculated by incorporating the RBC's and plasma values from hematocrits into the calculated total % of the dose in whole blood.

§ The total % of the dose in bone was calculated by assuming that the skeleton comprised 10% of the total body weight and that the distribution of radioactivity was the same in the femur and other bones. The calculated dose in bone was not included in total dose recovered (bone was counted with carcass).

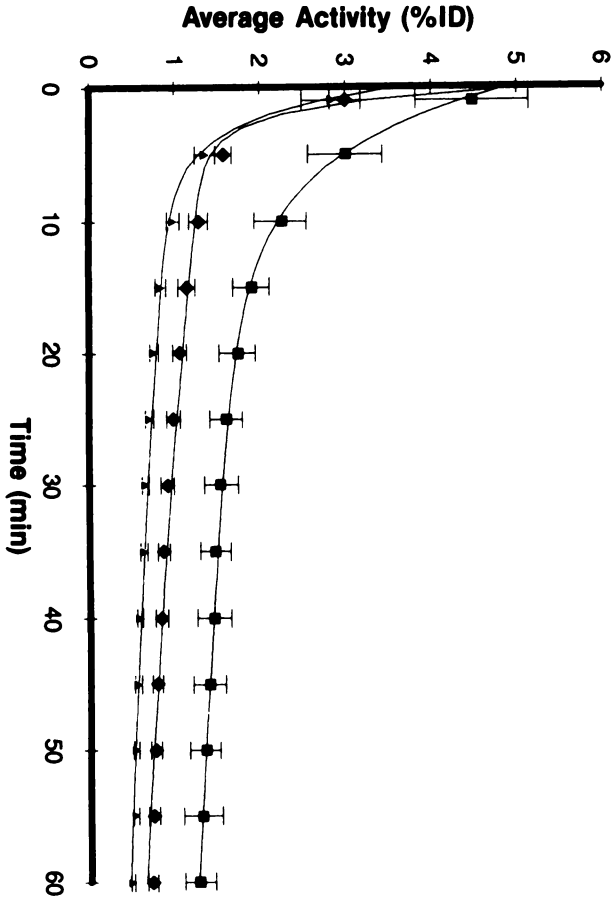

FIGURE 4
Clearance of [^{99m}]Tc-CDO-MeB from hearts of dog, guinea pig, and rat; average activity (% ID) vs. time (min) is shown for dog (n = 4), ■; guinea pig (n = 6), ◆; rat (n = 4), ▲; with respective fit functions of: $2.98\ e^{-0.194t} + 1.92\ e^{-0.0069t}$; $3.76\ e^{-0.725t} + 1.42\ e^{-0.0130t}$; and $2.57\ e^{-0.414t} + 1.03\ e^{-0.0134t}$.

The heart uptake of 3.44% ID for [^{99m}Tc]CDO-MeB versus 3.03% for ^{201}Tl at 1 min postinjection (Table 1) suggests high extraction of [^{99m}Tc]CDO-MeB by the rat myocardium. Using an isolated blood-perfused rabbit heart model Meerdink et al. showed that myocardial extraction of CDO-MeB (SQ 30217) is at least equal to if not greater than that of thallium (*22*). The extractions of CDO-MeB and Tl over a range of coronary blood flows (0.15–2.44 ml/min/g), ranged from 0.88 to 0.53 and 0.81 to 0.36, respectively.

The majority of the ^{99m}Tc-based cationic agents have shown marked species dependence of uptake. Although the rat model shows good uptake for all potential compounds tested, the clinical results were disappointing. The Tc(III) complexes $[^{99m}Tc(DMPE)_2Cl_2]^+$ and $[^{99m}Tc(DEPE)_2Cl_2]^+$ showed in humans no detectable myocardial uptake with low heart/liver ratios; and the Tc(I) complexes $[^{99m}Tc(DMPE)_3]^+$, $[^{99m}Tc(POM\text{-}POM)_3]^+$ and $[^{99m}Tc(TMP)_6]^+$ clear very slowly from the human blood (*11*). Thus for these complexes, the rat does not appear to be a good model for predicting the myocardial imaging characteristics in humans. Our results (Table 2) show that while the rat model gave similar uptakes for all the four compounds the guinea pig model gave poor uptakes for $Tc(DMPE)_2Cl_2^+$ and $Tc(DMPE)_3^+$, and good uptake for TcBIN and [^{99m}Tc] CDO-MeB. It has been reported that TcBIN gives efficacious images of the human heart (*23*), likewise [^{99m}Tc] CDO-MeB gives good image of the human heart (*24*); whereas $Tc(DMPE)_2Cl_2^+$ and $Tc(DMPE)_3^+$ have failed to give good images of the human heart (*8,10*). Thus, the guinea pig may be a better predictor of human myocardial uptake than the rat.

Though approximately two-thirds of the activity from the dog heart is cleared with a half-time of 3.6 min, the SPECT images starting 10 min after the injection clearly identified the perfusion defect in both the ischemic dogs studied. This suggests that faster clearance from the heart is not really a problem in obtaining SPECT images. Coleman et al. measured myocardial blood flows in a canine model using [^{99m}Tc]CDO-MeB, ^{201}Tl and ^{113}Sn-microspheres (*25*). There was an excellent correlation among the three methods over a wide

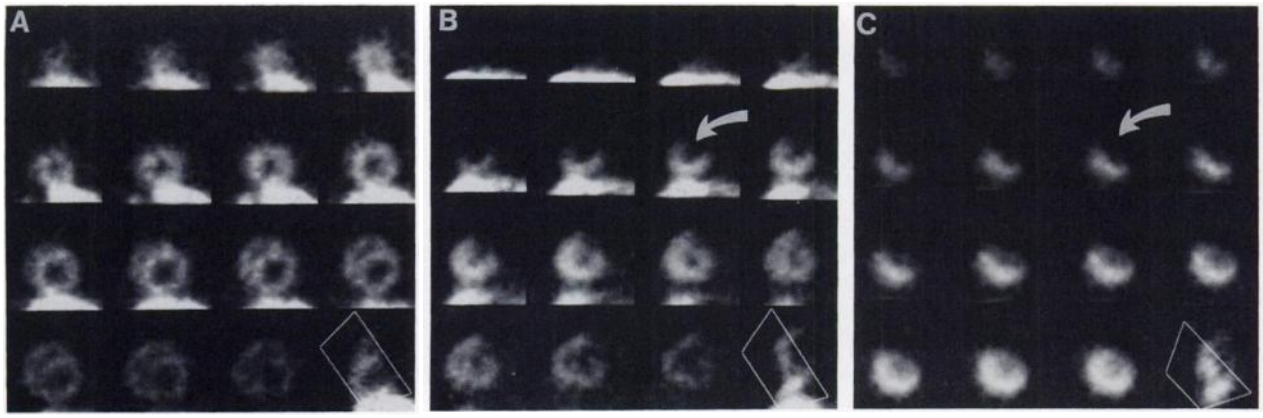

FIGURE 5
Short-axis oblique reconstructions comparing a normal dog heart (A) to myocardial ischemia models (B) and (C) involving the left descending coronary artery. In both (B) and (C) the anterior defect indicated by an arrow in frame 7 is apparent in frames 3 to 10.

range of flows, from 0.004 to 6.2 ml/min/g. These data indicate that [^{99m}Tc]CDO-MeB will indeed serve as a tracer for myocardial blood flow determinations.

Initial clinical studies using a kit formulation are promising (*24*). Clinically efficacious views of the myocardium could be obtained from 1 to 20 min after injection. The clearance characteristics of [^{99m}Tc]CDO-MeB are such that a repeat injection at rest or after drug intervention can be performed ~1hr after the first study.

The data in rats, guinea pigs, and dogs, and the findings from initial clinical studies indicate that [^{99m}Tc] CDO-MeB is a promising myocardial perfusion imaging agent in humans.

REFERENCES

1. Strauss HW, Pitt B. Thallium-201 as a myocardial imaging agent. *Semin Nucl Med* 1977; 7:49–58.
2. Pitt B, Strauss HW. Clinical application of myocardial imaging with thallium. In: Strauss HW, Pitt B, eds. *Cardiovascular nuclear medicine.* Second ed. St. Louis: C.V. Mosby, 1979:243–252.
3. Ritchie JL, Trobaugh BG, Hamilton GW, et al. Myocardial imaging with thallium-201 at rest and during exercise. Comparison with coronary arteriography and resting and stress electrocardiography. *Circulation* 1979; 56:66–71.
4. Gibson RS, Taylor GJ, Watson DD, et al. Predicting the extent and location of coronary artery disease during the early postinfarction period by quantitative thallium-201 scintigraphy. *Am J Cardiol* 1981; 47: 1010–1019.
5. Deutsch E, Bushong W, Glaven KA, et al. Heart imaging with cationic complexes of technetium. *Science* 1981; 214:85–86.
6. Deutsch E, Glavan KA, Sodd VJ, Nishiyama H, Ferguson DL, Lukes SJ. Cationic ^{99m}Tc complexes as potential myocardial imaging agent. *J Nucl Med* 1981; 22:897–907.
7. Eakins MN, Glavan KA, Kronauge JF, Neirinckx RD, LaTegola Graff M. The myocardial uptake and biodistribution of kit formulated, ^{99m}Tc-labeled cationic complex, $Tc(dmpe)_2Cl_2^+$. *J Lab Comp Radiopharm* 1982; 19:1457–1459.
8. Gerson MC, Deutsch EA, Nishiyama H, et al. Myocardial perfusion imaging with technetium-99m DMPE in man. *Eur J Nucl Med* 1983; 8:371–374.
9. Dudczak R, Angelberger P, Homan R, Kletter K, Schmoliner R, Frischauf H. Evaluation of ^{99m}Tc-dichloro bis(1,2-dimethylphosphino)ethane (^{99m}Tc-DMPE) for myocardial scintigraphy in man. *Eur J Nucl Med* 1983; 8:513–515.
10. Gerson MC, Deutsch EA, Libson KF, et al. Myocardial scintigraphy with ^{99m}Tc-tris-DMPE in man. *Eur J Nucl Med* 1984; 9:403–407.
11. Gerundini P, Savi A, Gilardi MC, et al. Evaluation in dogs and humans of three potential technetium-99m myocardial perfusion agents. *J Nucl Med* 1986; 27:409–416.
12. Sia STB, Holman BL, McKusick K, et al. The utilization of Tc-99m-TBI as a myocardial perfusion agent in exercise studies: comparison with Tl-201 thallous chloride and examination of its biodistribution in humans. *Eur J Nucl Med* 1986; 12:333–336.
13. Stirner H, Buell U, Kleinhaus E, Vebis R, Biedermann M. Tc-99m hexakis-(2-methoxy-isobutyl-isonitrile) (RP-30) vs ^{201}Tl. A quantitative comparison with SPECT in coronary heart disease (CHD) [Abstract]. *J Nucl Med* 1987; 28:620–621.
14. Treher EN, Gougoutas J, Malley M, Nunn AD, Unger SE. New technetium radiopharmaceuticals: boronic acid adducts of vicinal dioxime complexes. *J Label Comp Radiopharm* 1986; 23:118–120.
15. Nunn AD, Feld TA, Treher EN. Boronic acid adducts of technetium-99m dioxime complexes. United States Patent #4,705,849; Nov. 10, 1987.
16. Treher EN, Francesconi LC, Gougoutas JZ, Malley MF, Nunn AD. Mono-capped tris dioxime complexes of technetium (III): synthesis and structural characterization of $TcX(dioxime)_3B$-R(X = CL, Br; dioxime-dimethylglyoxime cyclohexanedionedioxime; R = CH_3, C_4H_9). *Inorg Chem*: 1989; 28:3411–3416.
17. Neirinckx RD, Glavan KA, Eakins MN, Kronauge JF. A kit procedure for the synthesis of the Tc-99m myocardial agent $Tc(DMPE)_2^+$. *Proceedings of the Third World Congress of Nuclear Medicine and Biology*, August 29–September 2, 1982, Paris, France. New York: Pergamon Press; 1982:698–701.
18. Abrams MJ, Davison A, Brodack JW, Jones AG, Costello CE, Pang H. Synthesis and characterization of hexakis(alkyl isocyanide) and hexakis(aryl isocyanide) complexes of technetium(I). *Inorg Chem* 1983; 22:2798–2800.
19. Snyder WS, Ford MR, Warner GG, Watson SB. "S" absorbed dose per unit accumulated activity for selected radionuclides and organs, *MIRD Pamphlet No. 11*. New York: The Society of Nuclear Medicine, 1975.
21. Baxenbaum HG, Riegelman S, Elashoff RM. Statistical estimations in pharmacokinetics. *J Pharmaco Biopharm* 1974; 2:123–148.
22. Meerdink DJ, Thurber M, Savage S, Leppo JA. Comparative myocardial extraction of two technetium-labeled boron oxime derivatives (SQ 30,217, SQ 32,014) and thallium [Abstract]. *J Nucl Med* 1988; 29:972.
23. Holman BL, Jones AG, Lister-James J, et al. A new Tc-99m-labeled myocardial imaging agent, hexakis (t-butylisonitrile)-technetium(I)[Tc-99m TBI]: Initial experience in the human. *J Nucl Med* 1984; 25:1350–1355.
24. Seldin DW, Johnson LL, Blood DK, et al. Myocardial perfusion imaging with technetium-99m SQ 30217: comparison with thallium-201 and coronary anatomy. *J Nucl Med* 1989; 30:312–319.
25. Coleman RE, Maturi M, Nunn AD, Eckelman WC, Cobb FR. Myocardial perfusion: comparison of SQ 30217, thallium-201 and microspheres in dogs [Abstract]. *J Nucl Med* 1987; 28:1080.